*Article*

# Average Generalized Ambiguity Function Analysis for Passive Bistatic SAR Systems Using PSK Modulating Signal

**Zhiping Yin [1], Lei Zhang [1], Jinbao Xie [1], Jun Yang [1], Guangsheng Deng [1] and Zhaoxian Zeng [2,*]**

[1] Academy of Photoelectric Technology, Hefei University of Technology, Hefei 230009, China; zpyin@hfut.edu.cn (Z.Y.); l_zhang_7@mail.hfut.edu.cn (L.Z.); xiejinbao@mail.hfut.edu.cn (J.X.); junyang@hfut.edu.cn (J.Y.); dgsh@hfut.edu.cn (G.D.)
[2] Beijing System Engineering Institute, Beijing, China
* Correspondence: josinzeng@126.com

**Abstract:** The formula of the Generalized Ambiguity Function (GAF) of passive bistatic SAR system using the non-cooperative illuminators which transmit PSK modulating signals is derived to analyze the spatial resolution of the system. The average GAF is introduced to remove the effect of particular sequence of symbols on resolution because the particular sequence of symbols is usually unpredictable before being received. The influence of the waveform parameters of the PSK modulating signals, such as length of the symbol sequence and roll-off factor, on spatial resolution is investigated by numerical simulation. It is confirmed that the influence of the length of the symbol sequence and roll-off factor is very slight but still exists.

**Keywords:** average generalized ambiguity function; passive bistatic SAR; PSK modulating signal; spatial resolution

## 1. Introduction

In recent years, the passive bistatic SAR/ISAR systems, which use the non-cooperative illuminators as the transmitters of opportunity, have drawn a lot of attention all over the world due to their prominent advantages in comparison to active radars, such as low cost, low probability of interception, flexible configuration, coverage characteristics and availability of rich illuminator sources [1, 2]. The passive radar imaging systems utilize broadcasting station [3], television transmitting tower [4], broadcasting satellite [5, 6], navigation satellite [7, 8], communication base station [9] and wireless networks [10, 11] as their illuminators with a bistatic geometry configuration. Phase shift keying (PSK) modulating signal is a potential source of illumination for passive imaging system due to its wide application in communication, radar, navigation and so on. The feasibility of two-dimensional imaging using scattered PSK-modulated communication signals was investigated by numerical simulation [12]. The passive SAR system based on digital video broadcasting satellites with QPSK modulation was studied using simulation [13] and experiment [14, 15], and its resolution capability was evaluated by the analysis of the wavenumber domain coverage in [13]. The ISAR image of a vehicle was obtained by passive radar system using DVB-S signals which implements QPSK modulation. In addition, PSK modulation techniques are widely used in the satellite navigation systems and the feasibility of the passive bistatic SAR systems has been theoretically and experimentally verified by using GPS [16], GLONASS [17, 18], GALILEO [7] and BDS [19] signals.

The spatial resolution is one key factor of the performance for SAR/ISAR imaging system. In traditional radar systems, the resolution which describes the capacity to separate two or more targets can be usually analyzed by calculating the ambiguity function. For SAR/ISAR imaging system, the generalized ambiguity function (GAF) was formed to evaluate the spatial resolution [20], which has been used in several papers to discuss the passive system resolution. In [21], the GAF of the bistatic SAR is deduced under narrowband assumption where the signal waveform was approximated by a Gaussian or rectangle pulse functions, and then the theoretical GAF equation of

Preprints (www.preprints.org) | NOT PEER-REVIEWED | Posted: 10 October 2017 doi:10.20944/preprints201710.0059.v1

the bistatic SAR was verified by an experimental passive system consisting of GLONASS satellites as transmitters and a fixed receiver [22]. In [23], the GAF of a multiple antennas multiple frequencies radar system was introduced, which described the effect of the signal bandwidth without the signal waveform on the resolution. Soon after this work, the experimental result of the GAF of multistatic SAR was achieved by combining reflected signals from several GLONASS satellites [24].

The present studies mentioned above about GAF of the passive SAR/ISAR systems mainly focused on the simplified signal model, and the effect of signal waveform on spatial resolution was ignored. In consideration of ambiguity function theory that the modulation signal waveform will impact on the system's ability to discriminate different targets in the delay-Doppler domain, it's very important to investigate the effect of signal waveform on profile of GAF to evaluate the performance of spatial resolution for the passive SAR/ISAR systems. Hence, this paper tries to study the GAF of the passive SAR system based on PSK modulating signals.

In this work, we derive the theoretical formula of the GAF of passive bistatic SAR system using the non-cooperative illuminators which transmit PSK modulating signal. The concept of average ambiguity function is introduced in order to analyze the resolution capability of the passive bistatic SAR system independently of the particular sequence of symbols of the transmitted signal, because the particular sequence of symbols is usually unpredictable before being received for passive system. Then, the influence of the waveform parameters of the PSK modulating signals, such as length of the symbol sequence and roll-off factor, on spatial resolution is discussed, while that of the code width, the main factor in determining the resolution which has discussed in [21], is ignored in this paper.

This paper is organized as follows. In Section 2 the geometry of the BISAR system is described and the transmitted signal model for the passive radar system is presented. In Section 3 we define and derive the average GAF of the BISAR system based on PSK modulating signals. In Section 4 the simulated analysis is presented in order to demonstrate the resolution capability of the system. Finally, concluding remarks are drawn in Section 5.

## 2. System and Signal

### *2.1 BISAR System Geometry*

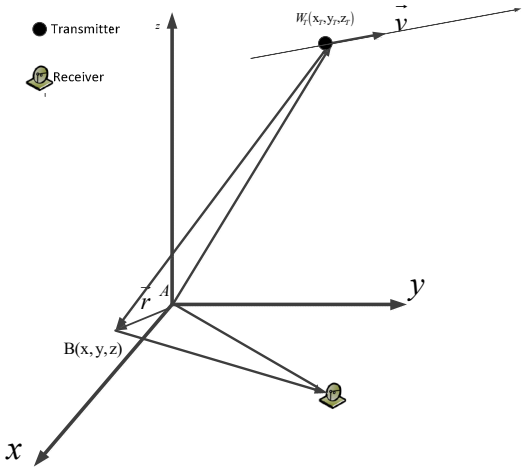


**Figure 1**. The BISAR geometry with a fixed receiver

Figure 1 shows a generalized geometry of a passive BISAR system. This configuration consists of a stationary target with the invariable scattering coefficient, a moving transmitter of opportunity, and a stationary receiver fixed on the ground. In this case, the distance between the transmitter and the target point is much greater than the distance between the receiver and the target point. In order to simplify the analysis, the three-dimensional coordinate system with the center of the target as origin is established. Vectors $\overrightarrow{W_T}$ and $\overrightarrow{W_R}$ denote the position coordinate of the transmitter and the

Preprints (www.preprints.org) | NOT PEER-REVIEWED | Posted: 10 October 2017 doi:10.20944/preprints201710.0059.v1

receiver respectively. Vector $\vec{v}$ is the velocity of the transmitter whose motion trajectory is a straight line during integration time.

There are two time variables that need considering in the BISAR system. One variable $t$ is the fast time, which describes the propagation of the ranging waveform. The other variable is the slow time $u$ that specifies the position of the receiver and the transmitter. In the system shown in Figure 1, only the position of the transmitter varies with the slow time $u$ and the motion is much slower than the propagation of the electromagnetic wave. Thus $\overrightarrow{W_T}$ is a function about $u$ and $\vec{v}$, and is represented at slow time $u$ as

$$\overrightarrow{W_T}(u) = \overrightarrow{W_T}(u_0) + \vec{v} \cdot u \,, \tag{1}$$

where $\overrightarrow{W_T}(u_0)$ is the position of the transmitter at the slow time instant $u = u_0$.

*2.2 Signal Model*

Assuming that the envelope and the carrier of the transmitted signal are $s(t)$ and $f_c$ respectively, the echo signal of the point target $A$ received by the receiver antenna can be represented as

$$s_A(t,u) = \sigma s(t-\tau_A) \mathrm{e}^{-j2\pi f_c \tau_A} e^{-j2\pi f_d^A (\mathrm{t}-\tau_A)} \,, \tag{2}$$

In this equation, $\sigma$ is the scattering coefficient of the target $A$, which is assumed to be constant and independent of the distance from the transmitter to the target. Furthermore, $\tau_A$ and $f_d^A$ are the time delay and the Doppler frequency respectively, which are the functions of slow time $u$. The equations about $\tau_A$ and $f_d^A$ are defined as

$$\tau_A(u) = \frac{\left|A - \overrightarrow{W_R}\right| + \left|A - \overrightarrow{W_T}(u)\right|}{c} \qquad f_d^A(u) = \frac{f_c}{c} \vec{v} \cdot \frac{A - \overrightarrow{W_T}(u)}{\left|A - \overrightarrow{W_T}(u)\right|} \,, \tag{3}$$

The PSK modulating signal transmitted by the illuminators of opportunity is pulse compression signal and is usually applied in the SAR systems in order to acquire the low probability of intercept. The expression of the unit energy complex envelope is defined as

$$s(t) = \frac{1}{\sqrt{N}} \sum_{n=0}^{N-1} c_n u_1(t - nT) \,, \tag{4}$$

where $c_n$ is the modulation code, which is usually pseudo-random or unpredictable, for the illuminator of opportunity and $N$ is the number of symbols. The pulse $u_1(t)$ is a rectangular pulse and $T$ is the width in the fast time domain. In order to reduce inter symbol interference, a delayed RRC filter is usually employed in systems as the pulse shaping filter. The equation of $u_1(t)$ is represented as

$$\begin{aligned} u_1(t) &= \frac{\sin(\frac{\pi t}{T}(1-\alpha)) + \frac{4\alpha t}{T}\cos(\frac{\pi t}{T}(1+\alpha))}{\frac{\pi t}{\sqrt{T}}[1-(\frac{4\alpha t}{T})^2]} \\ u_1(t=0) &= \frac{1}{\sqrt{T}}(1-\alpha+\frac{4\alpha}{\pi}) \\ u_1(t=\pm\frac{T}{4\alpha}) &= \frac{\alpha}{\sqrt{2T}}[(1+\frac{2}{\pi})\sin(\frac{\pi}{4\alpha}) + (1-\frac{2}{\pi})\cos(\frac{\pi}{4\alpha})] \end{aligned} \,, \tag{5}$$

where $\alpha$ is the roll-off factor of the filter, which lies in the interval [0,1] for all transmitters. Denoting the Fourier transform of the pulse $u_1(t)$ as $U(f)$, $|U(f)|^2$ can be defined as

Preprints (www.preprints.org) | NOT PEER-REVIEWED | Posted: 10 October 2017 doi:10.20944/preprints201710.0059.v1

$$|U(f)|^2=\begin{cases} T & |f|\le\dfrac{1-\alpha}{2T} \\ \dfrac{T}{2}[1+\cos(\dfrac{\pi T}{\alpha}(|f|-\dfrac{1-\alpha}{2T}))] & \dfrac{1+\alpha}{2T}\le|f|\le\dfrac{1+\alpha}{2T} \\ 0 & other \end{cases}, \tag{6}$$

Having presented the BISAR system geometry and the expression of the transmitted signals, the research now moves on to the study of the generalized ambiguity function in the following section.

## 3. Ambiguity Function of BISAR

The spatial resolution of the remote sensing system is one of the key parameters and is defined as the capacity to separate two or more targets in spatial domain. The ambiguity function (AF) is usually studied to obtain the resolution of the system, in terms of range and speed. In order to study the spatial resolution in SAR, the definition of radar AF has been extended to GAF by Tao Zeng, et al. [21] and the equation is represented as

$$\chi(\vec{r})=\iint s_A(t,u)s_B^*(t,u)dtdu\,, \tag{7}$$

where $s_A(t,u)$ and $s_B(t,u)$ are the complex envelopes of reflected signals from two point target located at the points $A$ and $B$, whose scattering coefficients are assumed as unit radar cross section. Point $A$ is the desired point scatterer to be evaluated, and $B$ is an arbitrary point scatterer in the vicinity of $A$. $\vec{r}$ is the distance vector from $A$ to $B$.

Different from the active radar which usually transmits deterministic signals, most of the received signals of passive radar are non-deterministic due to the non-cooperative of the illuminators. In the case of PSK modulating signals, the non-deterministic means the sequence of symbols is pseudo-random, such as the signals from navigation system, or unpredictable, such as the signals from communication system. In order to remove the impact of the non-deterministic of the sequence of symbols on the profile of GAF, the concept of the average ambiguity function is introduced here. The average ambiguity function defined by Cooper is generalized to the average GAF of the BISAR system, which is written as follow

$$A(\vec{r})=E\left\{\left|\chi(\vec{r})\right|^2\right\}=E\left\{\left|\iint s_A(t,u)s_B^*(t,u)dtdu\right|^2\right\}, \tag{8}$$

By substituting the expressions of the echo signals, the GAF of the system is represented as

$$\begin{aligned} A(\vec{r})=&\frac{\sigma^2}{N^2}\sum_{n=0}^{N-1}\sum_{n'=0}^{N-1}\sum_{k=0}^{N-1}\sum_{k'=0}^{N-1}E\{c_n\,c_{n'}^*c_k^*\,c_{k'}\}\\ &\times\iint u_1(t-nT-\tau_A)u_1^*(t-n'T-\tau_B)e^{j2\pi f_c(\tau_B-\tau_A)}e^{j2\pi(f_d^B-f_d^A)t}e^{-j2\pi(f_d^B\tau_B-f_d^A\tau_A)}dtdu\\ &\times\left(\iint u_1(t-kT-\tau_A)u_1^*(t-k'T-\tau_B)e^{j2\pi f_c(\tau_B-\tau_A)}e^{j2\pi(f_d^B-f_d^A)t}e^{-j2\pi(f_d^B\tau_B-f_d^A\tau_A)}dtdu\right)^* \end{aligned}, \tag{9}$$

where $\tau_A$ and $\tau_B$ are the time delay of the echo signals for target point $A$ and arbitrary point $B$ respectively, and the expectation $E\{\cdot\}$ is with respect to the transmitted modulation code $c_n$. All the transmitted pulses are independent and identically distributed across symbol indices, and $E\{\cdot\}$ can be written as below.

Preprints (www.preprints.org) | NOT PEER-REVIEWED | Posted: 10 October 2017 doi:10.20944/preprints201710.0059.v1

$$E\{c_n\, c_{n'}^{*} c_k^{*}\, c_{k'}\} = \begin{cases} 1, & n = n', k = k'; \\ 1 & n = k, n' = k', n \neq n'; \\ 0 & others \end{cases}, \tag{10}$$

Substituting the equation (10) and deducing this function from time domain to frequency domain in accordance with Fourier transform, the equation (9) can be converted into

$$\begin{aligned} A(\vec{r}) = \sigma^4 & \\ & \times \iint U(f - f_d^B + f_d^A) U^*(f) e^{j2\pi f(\tau_B - \tau_A)} e^{j2\pi f_c(\tau_B - \tau_A)} e^{-j2\pi(f_d^B \tau_B - f_d^A \tau_A)} df du \\ & \times \left( \iint U(f - f_d^B + f_d^A) U^*(f) e^{j2\pi f(\tau_B - \tau_A)} e^{j2\pi f_c(\tau_B - \tau_A)} e^{-j2\pi(f_d^B \tau_B - f_d^A \tau_A)} df du \right)^* \\ & + \frac{\sigma^4}{N^2} \sum_{n=0}^{N-1} \sum_{k=0, k\neq n}^{N-1} \\ & \left[ \iint U(f - f_d^B + f_d^A) U^*(f) e^{j2\pi f(\tau_B - \tau_A + (k-n)T)} e^{j2\pi f_c(\tau_B - \tau_A)} e^{-j2\pi(f_d^B \tau_B - f_d^A \tau_A)} df du \right. \\ & \left. \times \left( \iint U(f - f_d^B + f_d^A) U^*(f) e^{j2\pi f(\tau_B - \tau_A + (k-n)T)} e^{j2\pi f_c(\tau_B - \tau_A)} e^{-j2\pi(f_d^B \tau_B - f_d^A \tau_A)} df du \right)^* \right] \end{aligned}, \tag{11}$$

where $U(f)$ is the Fourier transform of the pulse $u_1(t)$. The delay difference between the received signals reflected by point $A$ and $B$ is defined as

$$\tau_B - \tau_A = \frac{\left|\overrightarrow{W_T}(u) - \vec{r}\right| + \left|\overrightarrow{W_R} - \vec{r}\right|}{c} - \frac{\left|\overrightarrow{W_T}(u)\right| + \left|\overrightarrow{W_R}\right|}{c}, \tag{12}$$

As is shown in Figure 1, the transmitter is usually far away from the target region and $|\vec{r}|$ is much smaller than the distance from the transmitter to the target. Denoting the unit vector in the direction of the receiver as $\vec{i}_T^A(u) = \vec{W}_T(u)/\left|\vec{W}_T(u)\right|$, the distance between the target and the receiver is presented as

$$\left|\overrightarrow{W_T}(u) - \vec{r}\right| = \left|\overrightarrow{W_T}(u)\right| - \overrightarrow{i_T}^A(u) \cdot \vec{r}, \tag{13}$$

Meanwhile, the receiver is not far away from the target region and $\left|\overrightarrow{W_R} - \vec{r}\right|$ needs to be calculated accurately. By considering the assumptions above, the delay difference $\tau_B - \tau_A$ is shown as

$$\tau_B - \tau_A = -\frac{\overrightarrow{i_T}^A(u) \cdot \vec{r}}{c} + \frac{\left|\overrightarrow{W_R} - \vec{r}\right| - \left|\overrightarrow{W_R}\right|}{c}, \tag{14}$$

Assuming the integration time was $T_0$ (i.e. $u \in [u_0 - T_0/2, u_0 + T_0/2\,]$) and denoting $u_0$ as the value at the midpoint of $T_0$, the equation (14) is approximated by its first-order Taylor expansion at $u = u_0$

$$\tau_B - \tau_A = -\frac{\overrightarrow{i_T}^A(u_0) \cdot \vec{r}}{c} + \frac{\left|\overrightarrow{W_R} - \vec{r}\right| - \left|\overrightarrow{W_R}\right|}{c} + \frac{\vec{r}}{c} \frac{d(-\overrightarrow{i_T}^A(u_0))}{du}(u - u_0), \tag{15}$$

Denoting $\tau_d$ and $f_d$ as the delay difference and the Doppler frequency when $u = u_0$, then

$$\tau_d = -\frac{\overrightarrow{i_T}^A(u_0) \cdot \vec{r}}{c} + \frac{\left|\overrightarrow{W_R} - \vec{r}\right| - \left|\overrightarrow{W_R}\right|}{c}, \quad f_d = f_c \frac{\vec{r}}{c} \frac{d(-\overrightarrow{i_T}^A(u_0))}{du}, \tag{16}$$

Therefore, the equation (14) can be simplified into

Preprints (www.preprints.org) | NOT PEER-REVIEWED | Posted: 10 October 2017 doi:10.20944/preprints201710.0059.v1

$$\tau_B - \tau_A = \tau_d + \frac{1}{f_c} \cdot f_d(u - u_0), \tag{17}$$

Meanwhile, the same approximation approach is applied and the phase term $f_d^B \tau_B - f_d^A \tau_A$ is approximated. The result of the simplification is represented as

$$\begin{aligned} f_d^B \tau_B - f_d^A \tau_A = & \frac{f_c \vec{v} \cdot \vec{r}}{c^2} + \frac{f_c \vec{v} \cdot (-\vec{i}_T^{\,A}(u_0))}{c^2} \left( \left| \overrightarrow{W_R} - \vec{r} \right| - \left| \overrightarrow{W_R} \right| \right) \\ & + \frac{\vec{v} \cdot \vec{r} \left( \left| \overrightarrow{W_R} - \vec{r} \right| - \left| \overrightarrow{W_R} \right| \right)}{c \left| \vec{r} \right|^2} f_d(u - u_0) \end{aligned}, \tag{18}$$

Considering the assumptions mentioned above and the characteristics of the signal which is narrowband, the equation (11) becomes

$$\begin{aligned} A(\vec{r}) = \sigma^4 & \left| \int e^{j2\pi f_d \left(1 - \frac{\vec{v} \cdot \vec{r} \left( \left| \overrightarrow{W_R} - \vec{r} \right| - \left| \overrightarrow{W_R} \right| \right)}{c \left| \vec{r} \right|^2}\right)(u - u_0)} du \right|^2 \\ & \times \left( \left| \int |U(f)|^2 e^{j2\pi f \tau_d} df \right|^2 + \frac{1}{N^2} \sum_{n=0}^{N-1} \sum_{k=0, k \neq n}^{N-1} \left| \int |U(f)|^2 e^{j2\pi f (\tau_d + (k-n)T)} df \right|^2 \right)' \\ & = K \bullet m(f_d) \bullet p(\tau_d) \end{aligned} \tag{19}$$

where $K$ is the coefficient which is irrelevant to $f$ and $u$, $m(f_d)$ is the integral of variable $u$ and $p(\tau_d)$ is the integral of variable $f$.

Equation (19) indicates that the average GAF of BISAR system using PSK modulating signal is presented as the production of two functions, $m(f_d)$ and $p(\tau_d)$, which is the same with the results in [21] . The azimuth resolution and its direction can be obtained from the function $m(f_d)$, which is mainly determined by motion of the transmitter and the integration time. Function $p(\tau_d)$, which contains the parameters of the PSK modulating signals including the code-width, the length of the symbols and the pulse shaped by RRC filter but excepting the particular sequence of symbols whose influence has been removed by the average processing for GAF, gives the radar spatial performance in the range domain. In a bistatic SAR system, the range resolution is in the direction of the bisector of the bistatic angle and the azimuth resolution's direction is specified by the equivalent motion direction. Generally, a more general resolution in any arbitrary direction of the X-Y plane is defined to analyze resolution capability of the system for the earth observation, so the resolution ellipse projected onto the X-Y plane is chosen in order to give tools to the radar system to evaluate the resolution capability [23]. $\delta_r$ and $\delta_a$ are defined in the direction of the projection of range and azimuth resolution onto the X-Y plane respectively. Figure 2 shows the projection of equation (19) for a BISAR system using a GPS satellite that will be used in the simulation in the next section. On the resolution ellipse, the maximum spatial resolution $\delta_{max}$ and minimum spatial resolution $\delta_{min}$ are along the major axis and the minor axis respectively and are usually applied to characterize the resolution capability. In this example, it can be clearly observed that the directions of projected range resolution $\delta_r$ and projected azimuth resolution $\delta_a$ don't overlap with that of the spatial resolution is $\delta_{max}$ or $\delta_{min}$ respectively, but the direction of $\delta_a$ is very colse to that of $\delta_{min}$.

Although the carrier frequency and signal bandwidth are the mainly decisive factors of the profile of the average GAF of BISAR system using PSK modulating signal, the length of the symbols and the pulse shaped by RRC filter may also have an impact on the average GAF of the system. Hence, the average GAF of BISAR system is calculated and discussed in the following section to evaluate the resolution performance of the system.

Preprints (www.preprints.org) | NOT PEER-REVIEWED | Posted: 10 October 2017 doi:10.20944/preprints201710.0059.v1

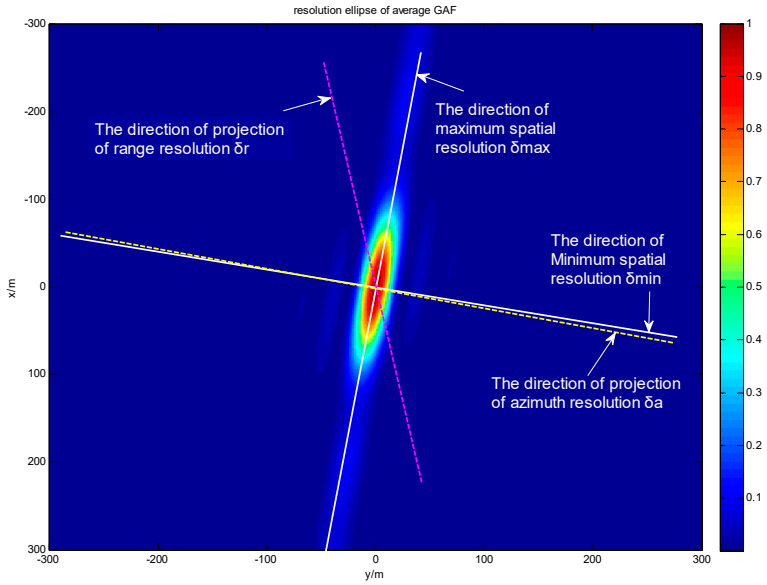


**Figure 2**. The resolution ellipse of the BISAR system and the directions of different resolution

## 4. Simulated Results and Analysis

In order to verify the average GAF of PSK modulation system mentioned in Section 3, the GAF of a passive BISAR system consisting of a GPS satellite as illuminator of opportunity and a receiver fixed on the ground is calculated by simulation. The GPS satellite runs over Hefei in one certain moment, and its parameters are shown in Table 1 and Table 2. It is assumed that the motion of the satellite is linear and the velocity is invariable during integration time. Meanwhile, the scattering coefficients of all reflectors within the imaging area are equal to one and independent of the distance from the transmitter to the target. Hence, an appropriate coordinate system is designed that X axis and Y axis is coincident with the east and north respectively, Z axis passed through the Earth's core, and X-Y plane is tangent to the Earth's surface. The target reflector to be analyzed is located at the center of the X-Y plane and B is an arbitrary point in the X-Y plane.

**Table. 1.** The fundamental parameters of GPS satellite

| Parameter | Symbol | Numerical Value |
|---|---|---|
| Carrier Frequency | $f_c$ | 1575.42MHz |
| Bandwidth of Signal | $B$ | 1.023MHz |
| Width of Pulse | $T$ | $1/1.023\times10^{-6}$ |
| Integration Time | $T_0$ | 60s |
| Velocity of Satellite | $\vec{v}$ | $(1.0962, -0.6366, -0.7552)\times10^4$ |
| Initial Position of Satellite | $\vec{W}_{T0}$ | (447075.2875, 20227806.07,1618341.826) |

**Table. 2**. The position of satellite as a function of integration time--$T_0 = 60s$

| Satellite | $\phi_e(u_0)$ | $\theta_e(u_0)$ | $\Delta\phi_e$ | $\Delta\theta_e$ |
|---|---|---|---|---|
| SAT15 | 300° | 78.5° | 1.91° | -0.167° |

### *4.1 GAF VS Average GAF*

The GAFs of the BISAR system using three kinds of pseudo-random symbols called M1, M2 and M3 with the number of the symbols of 1001 and the roll-off factor $\alpha$ of 0.22 are shown in Figure 3-5 respectively. The average GAF of the system with the same number of the symbols and roll-off

Preprints (www.preprints.org) | NOT PEER-REVIEWED | Posted: 10 October 2017 doi:10.20944/preprints201710.0059.v1

factor is also calculated and shown in Figure 6. In order to compare the resolution capability with each other, the resolution slices along the major and minor axis are plotted in Figure 7 and Figure 8.

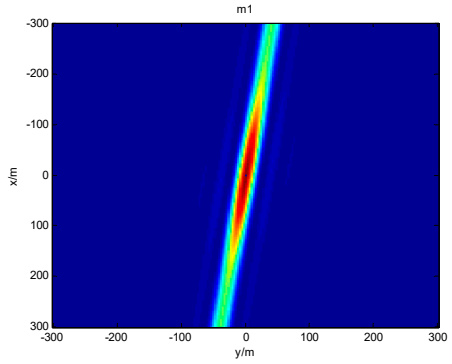


**Figure 3**. Generalized ambiguity function about M1

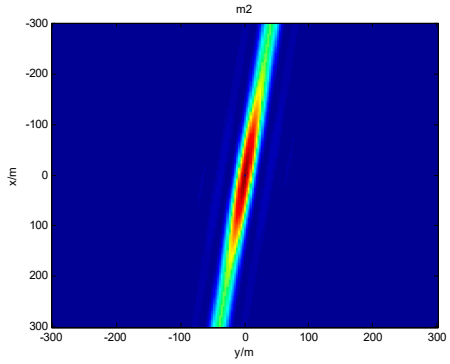


**Figure 4**. Generalized ambiguity function about M2

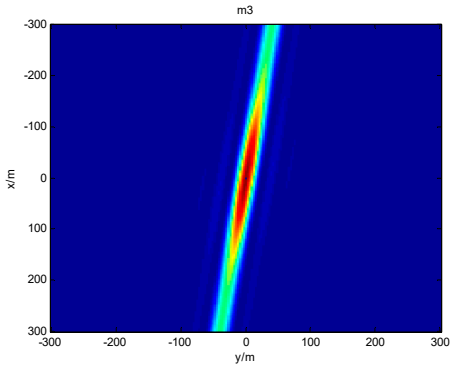


**Figure 5**. Generalized ambiguity function about M3

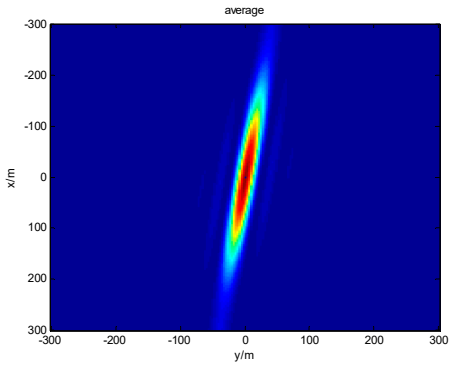


**Figure 6**. Average GAF of the BISAR system

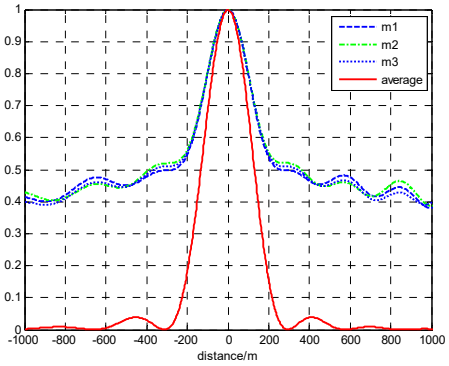


**Figure 7**. The resolution slice along major axis

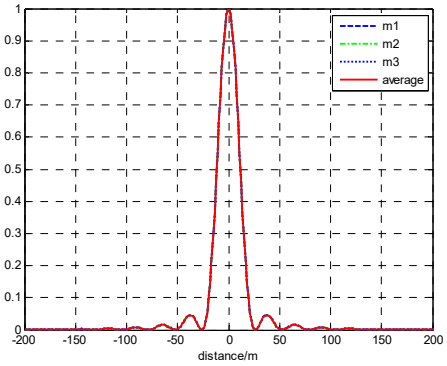


**Figure 8**. The resolution slice along minor axis

As shown in Figure 3, 4 and 5, it can be observed that the system based on different sequences with the same number of the symbols provides almost the same resolution ellipses, because these sequences are only different in the transmitted symbol sequence. The resolution slices along the major axis (Figure 7) demonstrate that their maximum spatial resolutions $\delta_{max}$ are exactly similar, especially for the mainlobe. The resolution slices along the minor axis (Figure 8) are identical, for the reason that the direction of $\delta_a$ and the direction of $\delta_{min}$ are basically consistent and the transmitted waveform has little impact on the azimuth resolution. Hence, the difference among their resolution ellipses caused by the different symbol sequence is very slight but still exists. Figure 6 shows the average GAF of the BISAR system. Comparing with Figure 3, 4 and 5, it is evident that the average GAF suppresses the sidelobe resulted from the independence of the particular symbol sequence. The independence of the particular symbol sequence means that the average GAF is more useful for evaluating the resolution of passive BISAR system, especially for the system that use the non-cooperative transmitters with unpredictable symbol sequences, such as PSK modulating communication transmitters.

Preprints (www.preprints.org) | NOT PEER-REVIEWED | Posted: 10 October 2017 doi:10.20944/preprints201710.0059.v1

### *4.2 The Impact of Number of Symbols*

It can be seen from the equation (19) that the number of symbols is one of the parameters for the BISAR system using PSK modulation. In this part, four sequences of different lengths are chosen to investigate the effect of length of the symbol sequence on the average GAFs. The roll-off factor is set to 0.22 for all four sequences. The resolution slices along the major axis and minor axis are shown in Figure 9 and Figure 10 respectively. It is obvious that the resolution slices along the major axis are identical except for small difference in sidelobe and the lower sidelobe will be obtained when using longer sequences. The resolution slices along the minor axis present the same curves which are overlapping each other. So the maximum and minimum spatial resolutions of the BISAR system based on four sequences of variable lengths are basically the same. The result indicates that the number of symbols have little influence on the resolution ellipse of BISAR system.

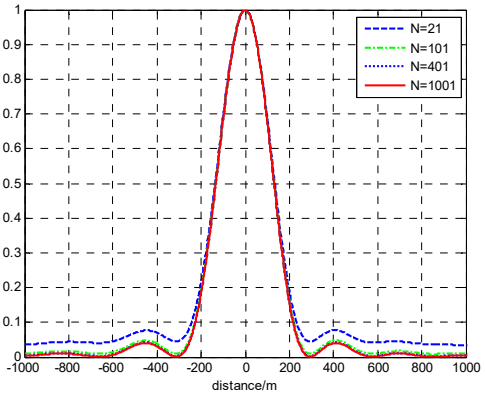


**Figure 9**. Resolution slice of average GAFs based on the length of sequence along major axis

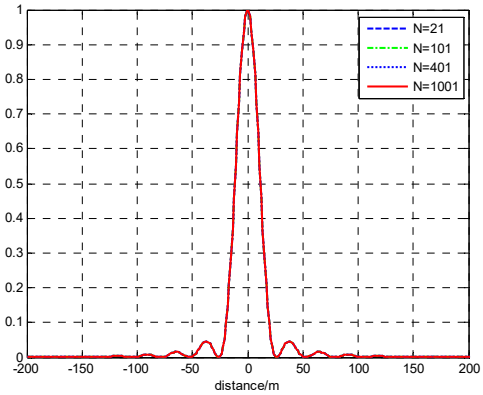


**Figure 10**. Resolution slice of average GAFs based on the length of sequence along minor axis

### *4.3 The Impact of Roll-off Factor*

As mentioned above, the pulse waveform $u_1(t)$ is obtained by applying a pulse shaping filter to each pulse to reduce inter symbol interference. In this work, a delayed RRC filter is applied and $\alpha$=0.2, 0.4, 0.6, 0.8 are chosen as the roll-off factor to calculate the average GAF in order to analyze the impact of the roll-off factor on the profile of average GAF. The resolution slices along the major axis and minor axis are shown in Figure 11 and 12 respectively. It is obvious that the minimum spatial resolutions $\delta_{min}$ are the same, and the maximum spatial resolutions $\delta_{max}$ present small difference for different roll-off factors, which causes different resolution ellipses. Hence, it can be observed that the BISAR system provides better resolution capability when the roll-off factor increases, because the increase can make the bandwidth of the signal expand simultaneously. We plot the -3dB contour of the spatial resolution along the major axis in Figure 13 to further study the effect of the roll-off factor on the resolution ellipse. The results in Figure 13 indicate that the PSK modulating signal whose roll-off factor is higher can have smaller maximum spatial resolution because of the tiny change of bandwidth due to filtering. While the value of the roll-off factor increases from 0.2 to 0.8, the maximum spatial resolution of the system decreases by 12.4% approximately. The increase means that the system can have better resolution capability.

Preprints (www.preprints.org) | NOT PEER-REVIEWED | Posted: 10 October 2017 doi:10.20944/preprints201710.0059.v1

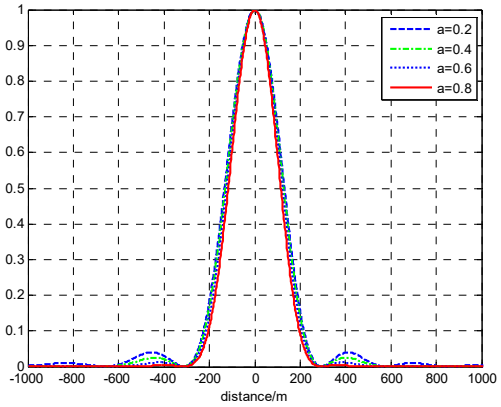


**Figure 11**. Resolution slice of average GAFs based on the roll-off factor along major axis

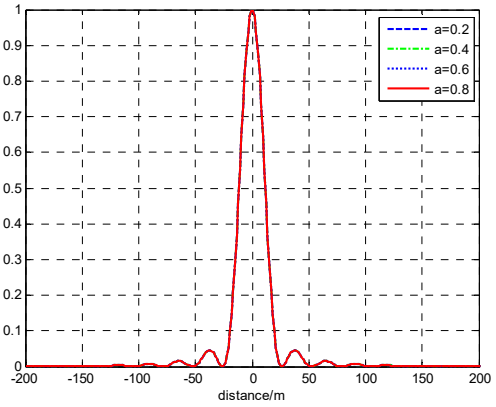


**Figure 12**. Resolution slice of average GAFs based on the roll-off factor along major axis

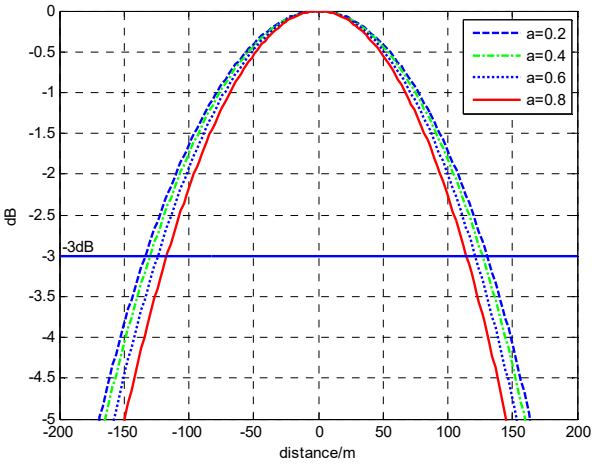


**Figure 13**. -3dB contour of the resolution slice based on the roll-off factor along major axis

## 5. Conclusion

In this paper, the resolution performance of the passive bistatic SAR system based on PSK modulating signal is investigated. The analytical form of the average GAF which is more useful for evaluating the resolution of passive BISAR system that use the non-cooperative transmitter with unpredictable symbol sequence is established and its formula in the case of PSK modulating signal used is deduce to evaluate the effect of the waveform on the resolution. The effect of the transmitted waveform on resolution is discussed in detail by numerical simulation. The conclusion can be drawn that the influence of the number of symbols and roll-off factor on resolution ellipse is very slight but still exists.

**Acknowledgments:** The work is supported by the General Program of National Natural Science Foundation of China under Grant No. 61401140. Moreover, the authors would like to thank Xinfei Lu for fruitful discussions.

**Author Contributions:** All authors contributed extensively to the work presented in this paper. Zhiping Yin and Lei Zhang designed the algorithm, analyzed the data and wrote the paper. Jinbao Xie designed and performed the simulations. Jun Yang, Guangsheng Deng, and Zhaoxian Zeng supervised its analysis, edited the manuscript and provided their valuable suggestions to improve this study.

**Conflicts of Interest:** The authors declare no conflict of interest

## References

[1] L. Maslikowski, P. Samczynski, M. Baczyk, P. Krysik, Passive bistatic SAR imaging — Challenges and limitations, IEEE Aerospace & Electronic Systems Magazine, 29(2014) 23-9.

[2] M. Martorella, E. Giusti, Theoretical foundation of passive bistatic ISAR imaging, Aerospace & Electronic Systems IEEE Transactions on, 50(2014) 1647-59.

[3] C. Prati, F. Rocca, D. Giancola, A.M. Guarnieri, Passive geosynchronous SAR system reusing backscattered digital audio broadcasting signals, IEEE Transactions on Geoscience & Remote Sensing, 36(2002) 1973-6.

[4] J. Wang, X. Zhang, Z. Bao, Passive Radar Imaging Algorithm Based on Subapertures Synthesis of Multiple Television Stations, Journal of Electronics & Information Technology, 29(2007) 1-4.

[5] D. Gromek, K. Kulpa, P. Samczyński, Experimental Results of Passive SAR Imaging Using DVB-T Illuminators of Opportunity, IEEE Geoscience & Remote Sensing Letters, 13(2016) 1124-8.

[6] W. Qiu, E. Giusti, A. Bacci, M. Martorella, F. Berizzi, H. Zhao, et al., Compressive sensing–based algorithm for passive bistatic ISAR with DVB-T signals, IEEE Transactions on Aerospace & Electronic Systems, 51(2015) 2166-80.

[7] M. Antoniou, Z. Hong, Z. Zeng, R. Zuo, Q. Zhang, M. Cherniakov, Passive bistatic synthetic aperture radar imaging with Galileo transmitters and a moving receiver: experimental demonstration, Iet Radar Sonar & Navigation, 7(2014) 985-93.

[8] H.C. Zeng, P.B. Wang, J. Chen, W. Liu, L.L. Ge, W. Yang, A Novel General Imaging Formation Algorithm for GNSS-Based Bistatic SAR, Sensors, 16(2016).

[9] A. Capria, E. Giusti, C. Moscardini, M. Conti, D. Petri, M. Martorella, et al., Multifunction imaging passive radar for harbour protection and navigation safety, IEEE Aerospace & Electronic Systems Magazine, 32(2017) 30-8.

[10] d.A. Gutierrez, J. R, J.A. Jackson, WiMAX OFDM for Passive SAR Ground Imaging, Aerospace & Electronic Systems IEEE Transactions on, 49(2013) 945-59.

[11] F. Colone, D. Pastina, P. Falcone, P. Lombardo, WiFi-Based Passive ISAR for High-Resolution Cross-Range Profiling of Moving Targets, IEEE Transactions on Geoscience & Remote Sensing, 52(2014) 3486-501.

[12] C. Sturm, S. Schulteis, W. Wiesbeck, Two-dimensional radar imaging with scattered PSK-modulated communication signals, Radar Conference, 2007 EuRAD 2007 European2007, pp. 134-7.

[13] C. Liu, T. Wang, L. Ding, W. Chen, Sparse imaging for passive radar system based on digital video broadcasting satellites, International Conference on Wireless Communications & Signal Processing2013, pp. 1-5.

[14] Z. Sun, T. Wang, T. Jiang, C. Chen, W. Chen, Analysis of the properties of DVB-S signal for passive radar application, International Conference on Wireless Communications & Signal Processing2013, pp. 1-5.

[15] M. Moscadelli, S. Brisken, V. Seidel, Passive radar imaging using DVB-S2, Radar Conference2017.

[16] F. Maussang, F. Daout, G. Ginolhac, F. Schmitt, GPS ISAR passive system characterization using Point Spread Function, New Trends for Environmental Monitoring Using Passive Systems2008, pp. 1-4.

[17] F. Liu, M. Antoniou, Z. Zeng, M. Cherniakov, Coherent Change Detection Using Passive GNSS-Based BSAR: Experimental Proof of Concept, IEEE Transactions on Geoscience & Remote Sensing, 51(2013) 4544-55.

[18] M. Antoniou, Z. Zeng, L. Feifeng, M. Cherniakov, Experimental Demonstration of Passive BSAR Imaging Using Navigation Satellites and a Fixed Receiver, IEEE Geoscience & Remote Sensing Letters, 9(2012) 477-81.

[19] T. Zeng, T. Zhang, W. Tian, C. Hu, X. Yang, Bistatic SAR imaging processing and experiment results using BeiDou-2/Compass-2 as illuminator of opportunity and a fixed receiver, Synthetic Aperture Radar2015, pp. 302-5.

[20] M. Skolnik, Radar Handbook, Third Edition2008.

[21] T. Zeng, M. Cherniakov, T. Long, Generalized approach to resolution analysis in BSAR, IEEE Transactions on Aerospace & Electronic Systems, 41(2005) 461-74.

 doi:10.20944/preprints201710.0059.v1

311 [22] F. Liu, M. Antoniou, Z. Zeng, M. Cherniakov, Point Spread Function Analysis for BSAR With GNSS
312 Transmitters and Long Dwell Times: Theory and Experimental Confirmation, IEEE Geoscience & Remote
313 Sensing Letters, 10(2013) 781-5.
314 [23] F. Daout, F. Schmitt, G. Ginolhac, P. Fargette, Multistatic and Multiple Frequency Imaging Resolution
315 Analysis-Application to GPS-Based Multistatic Radar, Aerospace & Electronic Systems IEEE Transactions on,
316 48(2012) 3042-57.
317 [24] F. Santi, M. Antoniou, D. Pastina, Point Spread Function Analysis for GNSS-Based Multistatic SAR, IEEE
318 Geoscience & Remote Sensing Letters, 12(2015) 304-8.